Bright novae

– Indications of the spectrum of MAXI J0158−744 –

Toshikazu Shigeyama,[1] Kentaro Wada,[1,2] Yukari Ohtani,[3]

[1] Research Center for the Early Universe, Graduate School of Science,
University of Tokyo, Bunkyo-ku, Tokyo 113-0033, Japan
[2] Department of Astronomy, Graduate School of Science, University of Tokyo, Bunkyo-ku, Tokyo 113-0033, Japan
[3] National Astronomical Observatory, Mitaka-shi, Tokyo 181-8588, Japan
E-mail(TS): shigeyama@resceu.s.u-tokyo.ac.jp

Abstract

We are trying to construct a theoretical model describing bright novae with luminosities exceeding 10^{39} erg s^{-1} in the context of a steady wind model emanating from the surface of a white dwarf. The motivation of this work originates from the discovery of a bright transient event MAXI J0158−744 in the Small Magellanic Cloud. We succeeded in reproducing the peculiar spectrum showing a strong Ne IX emission line at 0.92 keV with a large equivalent width and the absence of Ne X line at 1.02 keV and other emission lines from heavier ions like Mg and Al at higher energies by assuming a very fast wind accelerated above the photosphere. This is in contrast with the existing nova wind model which assumes acceleration below the photosphere. Thus we have extended the previous model to include the optically thin region by utilizing a flux-limited diffusion approximation. Though we can obtain solutions in which the wind is accelerated above the photosphere, the luminosity cannot be so high as observed. We will discuss possibilities to obtain more luminous solutions compatible with observed bright events including MAXI J0158−744.

Key words: novae — stars: winds —line: profiles — scattering — radiation: dynamics

1. MAXI J0158−744

A bright transient source MAXI J0158−744 was discovered by MAXI (Matsuoka et al. 2009) in the direction of the Small Magellanic Cloud on 2011 Nov. 11. Li et al. (2012) reported this discovery together with results of the follow-up observations by Swift and other optical telescopes. The detailed features of this object including the spectrum is given by Morii et al. (2013). The continuum was fitted by a black body spectrum with a temperature of $kT \sim 0.33$ keV. This object became as bright as $\sim 10^{40}$ erg s^{-1} at maximum and lasted for $\sim 10,000$ s. The inferred photospheric radius of a few thousand kilometer suggests that the emission originates from the surface of a white dwarf. Thus this transient phenomenon is a kind of nova explosions with an extremely short duration. Such a short duration indicates the mass of this white dwarf close to the Chandrasekhar limit. Thus the estimated luminosity clearly exceeds the Eddington limit.

The observed spectrum had a peculiar feature. There is a prominent emission line due to He-like Ne ions at 0.92 keV with an equivalent width of $0.32\ ^{+0.21}_{-0.11}$keV while no other lines were detected. This is strange because there should be, for example, a strong emission line due to H-like Ne ions with this observed photospheric temperature of $kT = 0.33$ keV. We tried to account for this peculiar spectrum by calculating radiative transfer of photons in an accelerating wind emanating from a white dwarf. In

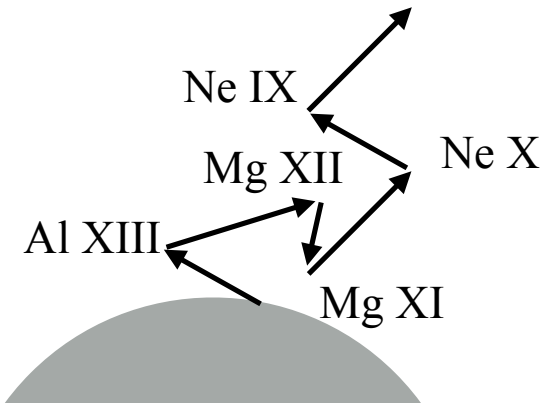

Fig. 1. Schematic view of line blanketing effects. See text for detail.

expanding spherical matter with positive velocity gradients, a photon scattered off a certain ion reduces its energy in the rest frames of any other ions at different places (Fig. 1). Thus a photon emitted by a certain ion with a higher transition energy (Al XIII in Fig. 1) is subsequently scattered off ions with lower transition energies (Mg and Ne ions). We expected that this line blanketing effects eliminate the other emission lines and have succeeded in reproducing the spectrum. Furthermore we are able to extract some information of this phenomenon such as the duration and the elemental abundances (Ohtani et al. 2014). We summarize the results in the next section.

1.1. Spectrum from accelerating nova wind

We have constructed a spherically symmetric steady wind model including optically thin regions. The velocity profile $v(r)$ is determined as a function of the radius r by the momentum conservations:

$$v\frac{dv}{dr} = \frac{\kappa L}{4\pi r^2 c}\left(1-\frac{L_{\rm Edd}}{L}\right), L_{\rm Edd} = \frac{4\pi cGM}{\kappa}, \quad (1)$$

where κ denotes the opacity, L the luminosity, c the speed of light, $L_{\rm Edd}$ the Eddington limit, G the gravitational constant, and M denotes the mass of the white dwarf. The fiducial value for L is 8×10^{39} erg s^{-1} and M is assumed to be 1.4 $M_\odot$. The solution of this equation can be obtained as,

$$v = \sqrt{\frac{\kappa L}{2\pi c R_0}\left(1-\frac{L_{\rm Edd}}{L}\right)\left(1-\frac{R_0}{r}\right)+v_0^2}, \quad (2)$$

where R_0 denotes the photospheric radius and $v_0 = v(R_0)$. The density profile $\rho(r)$ is determined from

$$\dot{M} = 4\pi r^2 \rho v, \quad (3)$$

where the constant mass loss rate $\dot{M}$ is determined to reproduce the observed photospheric radius of 2,300 km. To determine the position of the photosphere, we calculate the ionization states of ions by the photo-ionizing plasma package in XSTAR (Kallman & Bautista 2001). The mass loss rate thus determined is $1.4\times10^{-6}\,M_\odot$ yr^{-1}, which is about 2 orders of magnitude smaller than that for a typical classical nova. The terminal velocity becomes as high as 100,000 km s^{-1}. Note that this simple model does not specify the energy source and assumes the luminosity of the observed value. This is different from the steady wind model presented in the next section, in which the obtained luminosity is required to be caused by the CNO-cycle in the vicinity of the surface of a white dwarf.

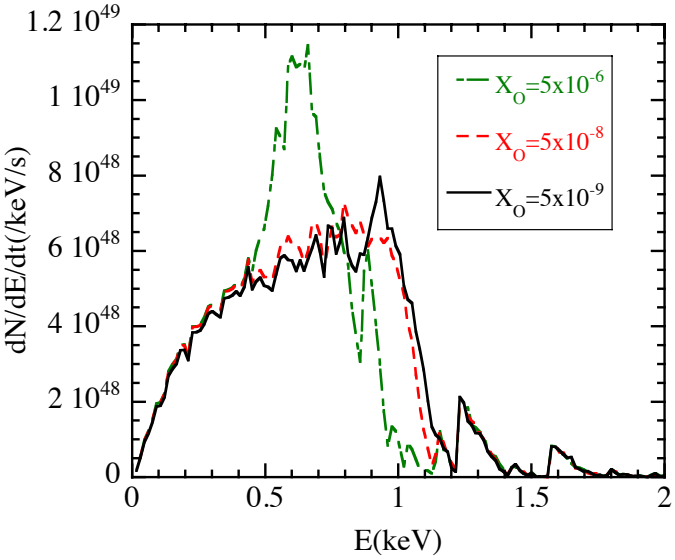

Fig. 2. Spectra with different oxygen abundances. The oxygen abundance should be smaller than 5×10^{-9} to reproduce the prominent emission line at 0.92 keV.

We calculate spectra by calculating radiative transfer of photons emitted from the photosphere by the Monte Carlo method (Ohtani et al. 2014). We find that emission lines at energies higher than 0.92 keV are eliminated by line blanketing effects. The same effect would eliminate the emission line at 0.92 keV if there were oxygen ions with $X_{\rm O} > 5\times10^{-9}$ in the wind because OVIII has a transition with an energy of 0.77 keV (see Fig. 2). The CNO cycle converts most of O to N in 2,400 s after its termination. We argued that this could explain the strong line at 0.92 keV. The abundance of Ne to reproduce the observed equivalent width needs to be $X_{\rm Ne} \sim 0.01$ or more. Thus the white dwarf is composed of O and Ne rather than C and O. In addition, the observed peculiar spectrum suggests that the wind is accelerated above the photosphere, which is at odds with the optically thick wind model Kato & Hachisu (1994) developed to reproduce light curves of novae till the beginning of the supersoft X-ray source phase. In this model, the sonic point resides below the photosphere and the velocity becomes almost constant before reaching the photosphere.

2. Steady wind model

To see whether there exist steady wind solutions in which the wind is accelerated above the photosphere, we extend the optically thick wind model to include the optically thin regions by using the M1 closure method (Levermore 1984) in the calculation of the radiative energy flux. Here we present a summary of Wada & Shigeyama (2017) in which winds from CO white dwarfs are explored.

Governing equations are the conservations of the mass,

the momentum, and the energy given by,

$$4\pi r^2 \rho v = \dot{M}, \tag{4}$$

$$\rho v \frac{dv}{dr} + \frac{dp_{\rm g}}{dr} = -\frac{GM\rho}{r^2} + \frac{\kappa \rho F_0}{c}, \tag{5}$$

$$\frac{1}{r^2}\frac{d}{dr}\left(r^2 v\left(e_{\rm g} + \frac{\rho v^2}{2} - \frac{GM\rho}{r} + p_{\rm g} + P_0 + E_0\right)\right)$$

$$+\frac{1}{r^2}\frac{d}{dr}\left(r^2 F_0\right) = \rho\epsilon, \tag{6}$$

where $p_{\rm g}$ the pressure due to ideal gas, G the gravitational constant, κ the opacity, F_0 the radiative flux in the rest frame of matter, c the speed of light, $e_{\rm g}$ denotes the energy density of gas, P_0 the radiation pressure, ϵ the energy generation rate due to nuclear reactions, E_0 is the energy density of radiation. Here the subscript 0 indicates the quantity in the rest frame of matter.

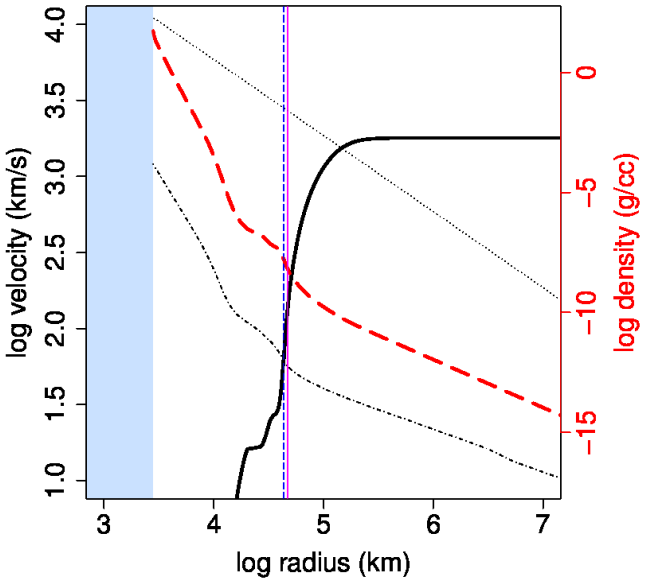

Fig. 3. Velocity (solid black line) and density (dashed red line) as functions of the radial coordinate for a nova wind model with a white dwarf mass of $M = 1.3\,M_\odot$, mass loss rate of $\dot{M} = 3.895 \times 10^{-7} M_\odot {\rm yr}^{-1}$, and luminosity of $L_\infty = 2.275 \times 10^{38}\,{\rm ergs}^{-1}$. The thin black lines denote escape velocity (dotted) and sound speed (dot dashed) respectively. The vertical dashed line indicates the radius of the critical sonic point and the vertical solid line the photosphere.

The opacity κ is calculated using the opacity table from OPAL (Iglesias & Rogers 1996) for a given chemical composition. The chemical composition in the wind is assumed to be uniform and constant: We set the mass fractions of hydrogen to $X_{\rm H} = 0.35$, helium $X_{\rm He} = 0.33$, heavy elements $Z = 0.02$, and the extra mass fractions

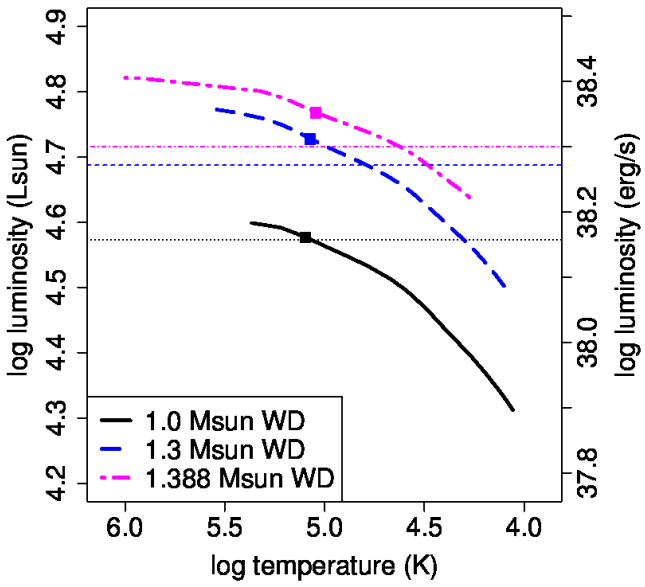

Fig. 4. Evolutions of luminosity and temperature of the photosphere in the HR diagram for white dwarfs with three different masses. Each filled square on a line represents the maximum luminosity and photospheric temperature attained by the corresponding optically thick wind model for each white dwarf.

of CNO elements that are not included in Z is set to $dX_{\rm CNO} = 0.30$.

The energy source of a nova is nuclear fusion reactions on the surface of a white dwarf, primarily CNO-cycle reactions. Instead of solving nuclear reaction network equations, we use approximate formulae of the energy generation rates for pp-chain, CNO-cycle, and triple alpha reactions as functions of the temperature T, the mass density, and the mass fractions of elements (Kippenhahn et al. 2012). We have denoted the sum of these three rates as ϵ in equation (6).

We numerically integrate the above three equations from a point far beyond the photosphere ($r = 10^9$ km) to the surface of a white dwarf with a given mass M by the 4th order classical Runge-Kutta method with a step size of $\Delta \ln r = 0.001$. The boundary conditions are: i) a given luminosity at $r = 10^9$ km, ii) the luminosity vanishing at the surface of the white dwarf. The other two are given by the mass loss rate $\dot{M}$ and the terminal velocity v_∞ (specified at $r = 10^9$ km). We use a shooting method repeating the integrations with various pairs of $\dot{M}$ and v_∞ to seek a solution that smoothly passes the critical sonic point and reaches the surface of the white dwarf with a vanishing luminosity. Thus the mass loss rate is obtained as an eigen-value to satisfy the boundary conditions.

We have succeeded in obtaining wind solutions with very small mass loss rates, which may describe the early super-soft X-ray source phases of novae (Fig. 3). In this phase, the bolometric luminosity of a nova becomes higher than before, the sonic point moves very close to the photosphere, and the wind is accelerated above the photosphere. On the other hand, we are not able to obtain a solution with a luminosity as high as 10^{39} erg s^{-1} even for a white dwarf with a mass close to the Chandrasekhar limit (see Fig. 4). Though there are transonic solutions with such high luminosities, none of them satisfies the inner boundary conditions. The terminal velocities are a few thousand km s^{-1} at most (Fig. 5), which is a factor of a few tens smaller than that required to reproduce the observed spectrum of MAXI J0158−744.

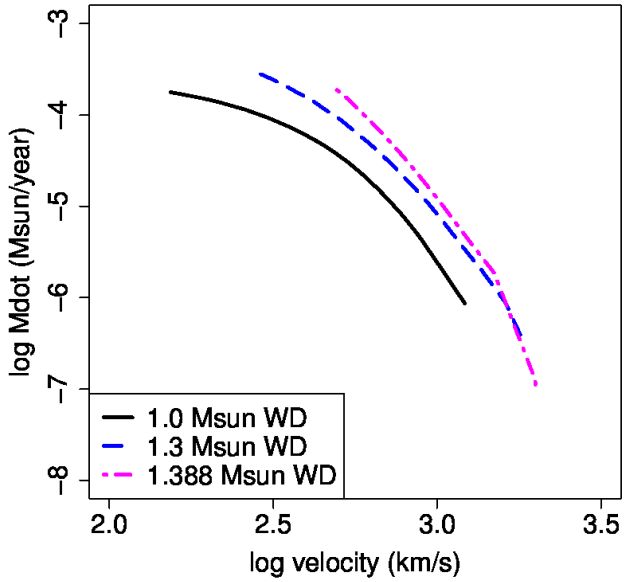

Fig. 5. Sequences of steady state solutions in the parameter space of the mass loss rate $\dot{M}$ and the terminal velocity v_∞. The thick solid line (black), the thick dashed line (blue), and the thick dot dashed line (magenta) denote models with white dwarf masses of $M = 1.0\,M_\odot$, 1.3 $M_\odot$, and 1.388 $M_\odot$, respectively.

3. Remaining problems

As shown in §1., the peculiar spectrum of MAXI J0158−744 indicates that matter in the wind is accelerated above the photosphere. The positive gradient of the velocity enables the line blanketing to eliminate emission lines at energies higher than 0.92 keV. On the other hand, the paucity of O ions in the wind as a result of the CNO cycle prevents the same mechanism from reducing the observed emission line at 0.92 keV. Since the current optically thick wind model can not deal with wind solutions in which the matter is accelerated above the photosphere, we have extended the model to include the optically thin region by introducing the M1-closure method. Though we obtain solutions in which the wind is accelerated above the photosphere, the maximum luminosity is far (more than a factor of 10) below that of MAXI J0158−744. As a result, the velocity and its gradient in these steady models are not sufficiently high for line blanketing effects to block photons with higher energies.

The observed values of the photospheric velocities and luminosities together with the short duration of MAXI J0158−744 indicate the mass of the white dwarf is close to the Chandrasekhar limit. A massive white dwarf composed of O and Ne rather than C and O is likely to reproduce the peculiar spectrum with a strong Ne emission line. With such a massive white dwarf, explosive thermonuclear runaway of the CNO-cycle might lead to luminosities much higher than those attained by steady state solutions investigated here. To explore such non-steady behaviors, we may need to integrate hydrodynamical equations with respect to time for periods much longer than the free-fall time scale at the surface of the white dwarf, which may need a significant improvement in the existing hydrodynamical codes to simultaneously trace explosive winds and nearly hydrostatic states of a white dwarf for a long period. Otherwise, we need to properly set boundary conditions at the surface of the white dwarf and calculate only the evolution of winds, though we do not know appropriate boundary conditions.

References

Iglesias, C. A., & Rogers, F. J. 1996, ApJ, 464, 943

Kallman, T., & Bautista, M. 2001, ApJS, 133, 221

Kato, M., & Hachisu, I. 1994, ApJ, 437, 802

Kippenhahn, R., Weigert, A., & Weiss, A. 2012, Stellar Structure and Evolution: Astronomy and Astrophysics Library. ISBN 978-3-642-30255-8. Springer-Verlag Berlin Heidelberg, 2012

Levermore, C. D. 1984, J. Quant. Spectrosc. Radiat. Transfer, 31, 149

Li, K. L., Kong, A. K. H., Charles, P. A., et al. 2012, ApJ, 761, 99

Morii, M., Tomida, H., Kimura, M., et al. 2013, ApJ, 779, 118

Matsuoka, M. et al. 2009, PASJ, 61, 999

Ohtani, Y., Morii, M., & Shigeyama, T. 2014, ApJ, 787, 165

Sugizaki, M. et al. 2011, PASJ, 63, 635

Wada, K., & Shigeyama, T. 2017, PASJ, submitted